



# INFLUENCE OF ADDITIVE MANUFACTURING ON ACOUSTIC METAMATERIALS PERFORMANCE: A CASE STUDY

Gioia Fusaro<sup>1\*</sup>

Luca Barbaresi<sup>1</sup>

Matteo Cingolani<sup>1</sup>,

Massimo Garai<sup>1</sup>

Edoardo Ida<sup>1</sup>

Andrea Prato<sup>2</sup>

Alessandro Schiavi<sup>2</sup>

<sup>1</sup> Department of Industrial Engineering, University of Bologna, Viale Risorgimento 2, Bologna, 40136, Italy

<sup>2</sup> INRiM – National Institute of Metrological Research, Division of Applied Metrology and Engineering, Torino, Italy

## ABSTRACT

Research on metamaterials relies on the rapid prototyping of samples implementing all geometrical details suggested by analytical or numerical studies. Therefore, precision in the realization of this geometry is vital for obtaining an acoustic result coherent with the analytical and numerical design. Additive manufacturing (AM) is the main technique in acoustic metamaterials (AMMs) prototyping, and so far, it has displayed interesting properties for quickly reproducing the geometries addressing specific resonance frequencies. However, AM parameters are generally not intended precisely for acoustic purposes, which may lead to a mismatch between the expected analytical or numerical results. In this study, AM parameters have been investigated to define the optimal printing configuration of a coiled-up resonator (as an example of AMM). Three printing techniques - Fused deposition modelling (FDM), Stereolithography (SLA), and Selective Laser Melting (SLM) - and four materials - PLA, PETGg, Resin, and Steel - have been investigated, due to their popularity among academic and private researchers. The sound absorption coefficient of each sample has been measured experimentally in two Italian research laboratories (INRiM Turin and University of Bologna). Next, the experimental results were compared to the analytical and numerical ones considering the impact of five specific parameters: Printing

velocity, Printing layer height, Filling density, Internal surface Roughness, and Internal surface porosity. The SLA/Resin combination performed better overall; however, properly set FDM and PETGg can achieve nearly the same acoustic precision in a cheaper and faster way. It is expected that these findings could be replicated for other AMMs.

**Keywords:** resonators; acoustic metamaterials; additive manufacturing; 3D printing; Sound Absorption.

## 1. INTRODUCTION

Acoustic metamaterials are becoming an effective alternative to traditional sound-insulating, absorbing and diffusing materials in the design of complex acoustic systems [1], [2].

The control of sound absorption and reflection, particularly at low frequencies or in specific narrow frequency bands (which generally require the use of bulky materials or systems), can be achieved by exploiting resonant structures and cavities with a special shape and small dimensions, such as a spiral resonator. Specifically, a spiral resonator is a classic Helmholtz resonator, already described in 1863 [3] with an elongated, coiled-up cavity. This geometric configuration allows the resonator to force an incident field of elastic waves (such as sound pressure waves) to behave in a way not found in nature or beyond what is possible with conventional materials, extending the material concept and improving its properties [4]. In this sense, a spiral resonator can be regarded as an "acoustic metamaterial", or better as a unit cell for an "acoustic metasurface" [5]), being

\*Corresponding author: [gioia.fusaro@unibo.it](mailto:gioia.fusaro@unibo.it)

Copyright: ©2023 First author et al. This is an open-access article distributed under the terms of the Creative Commons Attribution 3.0 Unported License, which permits unrestricted use, distribution, and reproduction in any medium, provided the original author and source are credited.

an artificially structured material, designed with the appropriate shape, size and arrangement.

On the other side, additive manufacturing is a reliable method widely used in the acoustic engineering research community [6], [7] through various techniques which are characterised by several 3D printing set-ups affecting the product quality [8], [9]. However, there are no specific guidelines in terms of 3D printing set-up implications with the performance of the prototype relying on the provisional expected result.

For these reasons, the present parametric and comparative investigation aims to determine whether, for spiral resonators, there may be an optimal configuration of techniques and materials for AM that can best approximate the designed analytical and numerical result. Firstly, Stinson's analytical model [10] coupled with a numerical analysis using the finite element method (FEM) [11] under measurement-like conditions provided an initial predicted result of the sound absorption coefficient. Secondly, a series of AM techniques (FDM, SLA and Selective Laser Melting, SLM) and 3D printing materials (PLA, PETG, Resin, flexible resin and stainless Steel) were used to produce the spiral resonator with various 3D printing set-ups (see Figure 1).

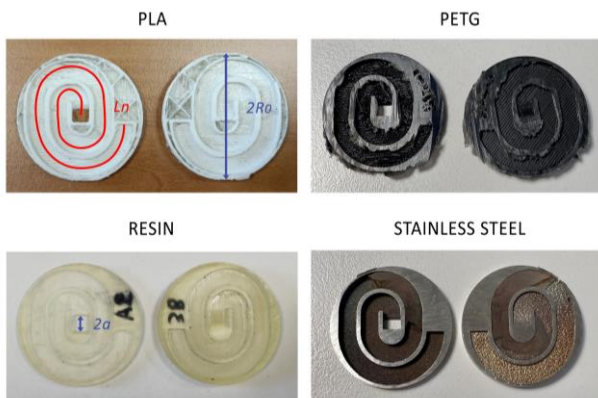


**Figure 1** 3D-printed prototypes in FDM-PLA, FDM-PETg, SLA-Resin and SLM-Stainless Steel, cut in half to show the upper (left) and lower (right) faces.

## 2. METHODS

### 2.1 Analytical and Numerical provisional study

Among sound absorbers based on the Helmholtz resonance principle, coiled-up resonators have been widely used due to their tenability and suitability for metasurfaces applications [12], [13]. For this reason, they were selected in this research to investigate the accuracy of different 3D printing materials and methods in reproducing the expected analytical and numerical results. Specifically, the geometrical model of coiled-up resonators that will be used has already been discussed in previously published papers [11], [14].

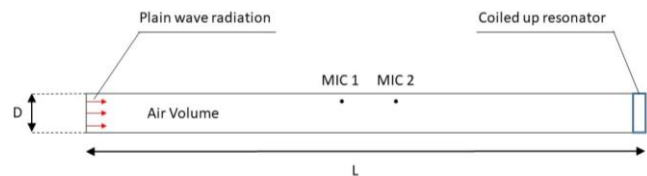


**Figure 2** Schematic of the geometry and the boundary conditions

In order to assess the analytical results and implement the metamaterial geometry through parametric sweeps, numerical models helped setting up a reference  $\alpha$ -value in reference conditions ( $T = 20 \text{ }^\circ\text{C}$ ) through the commercial software COMSOL Multiphysics [11], [15]. In order to reproduce the experimental impedance tube's transfer-function method, the boundary conditions of the numerical model are characterised by plane wave radiation (to simulate the loudspeaker) at the side of the impedance tube opposite to the coiled-up resonator, with a prescribed sound pressure amplitude of 1 Pa (see Figure 2). Furthermore, all the geometry is characterised as sound hard boundary conditions imposing null displacements along the axial direction concerning the tube. Finally, the mesh size has been defined through the standard FEM criterion for acoustic models to obtain at least six elements for the smallest wavelength, considering the maximum frequency of 4000 Hz, according to convergence recommendations [16].

### 2.2 Experimental assessment

Two impedance tubes (one at the National Institute of Metrology, INRIM, and another at the DIN laboratories, University of Bologna) were used to assess the analytical and numerical results defined as "provisional results" of each 3D printing configuration and determine which

combination of printing techniques and materials was the most effective to accurately reproduce the expected acoustic performance. Experimental acoustic absorption ( $\alpha_n$ ) values were analysed in the whole frequency spectrum (300-4000 Hz) considered at  $T = 20^\circ\text{C}$  [17]. More information on the systems set-up can be found in a previous article [14].

### 3. STUDY OF 3D PRINTING PARAMETERS

Five prototypes have been produced through Fused Deposition Modelling (FDM), Stereolithography (SLA), and Selective Laser Melting (SLM). In the first method, a specific material (PLA or PETG) filament is fused through a nozzle and deposited on the printing platform following specific geometry and layering inputs. In the second method (SLA), the liquid material (resin), constrained in a container, is polymerised through UV light following a specific geometry. Finally, the third method (SLM) generates a designed geometry by melting a stainless steel powder.

As highlighted from Figure 1 in this research, various combinations of printing settings are explored to assess the influence of the manufacturing process on the acoustic properties of the AMM geometry under study. The samples have been cut in half to make clearer the results of each method of printing; the upper (left) and lower (right) sides are displayed in Figure 1. Specific attention should be addressed to the resulting volumes, defined as a volume within the prototype geometry that does not have a specific characterisation (e.g., the volume enclosed in a cylinder) and for which a filling density can be set up (with different degrees of customizability). Another important feature shown in Figure 1 is the inner filaments layering characterisation, which depends on the printing Speed and Quality of the printing machines' set-ups [14].

## 4. RESULTS

### 4.1 Sound absorption coefficient from different AM technologies and materials

Among the various 3D printing set-ups tested to reproduce the spiral resonator geometry, the prototype in SLM Steel is the one with the worst performance (due to a metal dust occlusion inside the resonator cavity, which impaired its performance). The Prototype in SLA Resin is the one with the best performance, given the extreme accuracy in reproducing the geometry in terms of volume, thickness, and surface homogeneity (limited

roughness). Finally, the two FDM PLA and PETG samples have a significantly different result, even though they were made with the same technique, as different print set-ups were selected. The difference is in fact due to the variable parameters of Printing Speed and Quality setting, which determine the surface characterisation of the inner wall of the resonant cavity and can cause, if improperly chosen, a deviation from the predicted (analytical and/or numerical) value of the sound absorption coefficient. The optimal combination of these two parameters turns out to be the "slow-fine" one (see Figure 3).

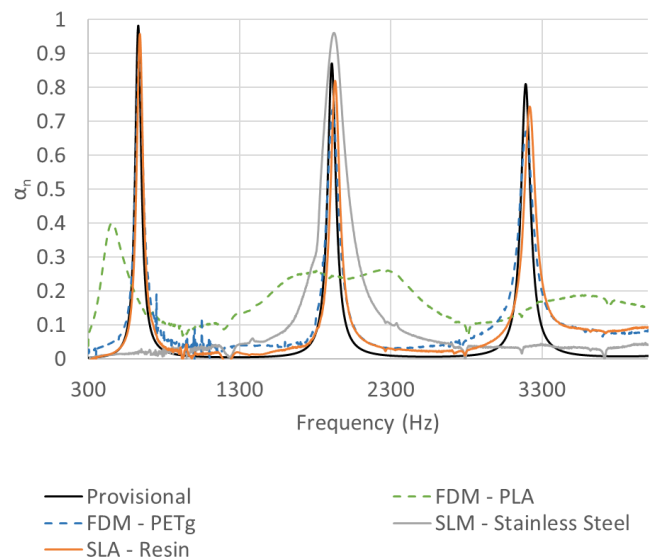


**Figure 3** – Predicted normal incidence sound absorption coefficient of samples of FDM - PLA and PETg, of SLM - Stainless Steel and SLA - Resin.

### 4.2 FDM set up investigation

Two of the samples involved in the present work were produced with FDM technology, which is one of the most popular additive manufacturing technologies for several reasons [18] (more information can be found in [14]). In particular, for the Flashforge Creator 3 and PETg combination, the speed parameters (Solid layer speed) and quality parameters (N. of top and bottom solid layers and Layer height) were involved in an optimisation process, keeping the other settings constant (see Table 1). Given several circular features in the specimens, a higher speed usually produces less accurate curvilinear features; thus, the faster the process, the worst the specimen is expected to be. Flashforge Creator 3 can produce components by depositing  $50\ \mu\text{m}$  thick

layers of thermoplastic material, with an 11  $\mu\text{m}$  horizontal positioning resolution within a layer. Simple stepper motors drive the Cartesian mechanical architecture that displaces the extruder nozzle without feedback control on the position of the nozzle. Thus, the manufacturing processes' absolute accuracy is influenced by the printing material (some thermoplastic polymers exhibit severe shrinkage and deformation after extrusion) and by the print-process setup [19]. In a previous article, the authors proved that the optimal printing set-up for achieving experimentally the provisional results was with slow printing speed (30 mm/s) and fine quality printing (layer height = 0.12 mm) [14].

**Table 1** – Constant or variable printing parameters

Constant parameters	Value
Extruder temperature ( $^{\circ}\text{C}$ )	225
Infill	Gyroid (3D infill)
Base speed (mm/s)	50
Outline speed (mm/s)	15
Solid layer speed (mm/s)	30
Infill speed (mm/s)	45
N. of top and bottom solid layers	4
Layer height (mm)	0.12
Variable parameters	Values
Infill density (%)	10, 20, 30, 40, 50

Fast printing setup (solid layer speed of 50 mm/s) resulted in a non-parallel deposition direction to the printing bottom layer caused by a deformation of the filament section while solidifying (not circular as expected) (see Fusaro et al. [14]). Moreover, coarse quality settings (2 top and bottom solid layers combined with a layer height of 0.3 mm) caused the appearance of macro porous on the surface of adherence between two layers overlapping. These features significantly impact the geometry and, therefore, the performance of the experimental prototype compared to the provisional results. So in this study, printing speed and quality were kept constant, while particular attention was paid to different infill density impact on the experimental results of  $\alpha_n$ .

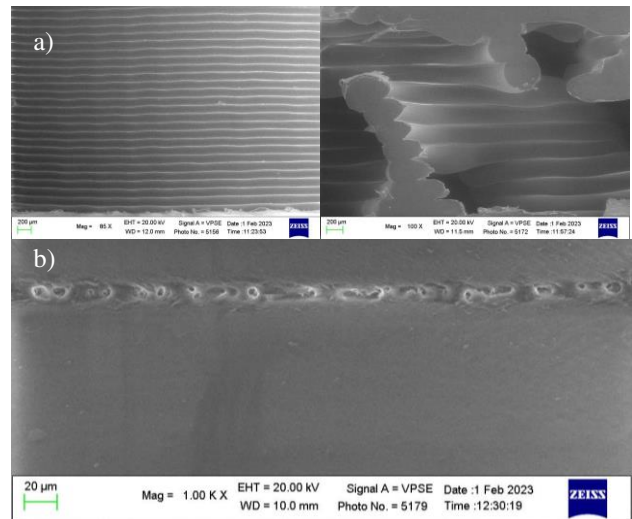


**Figure 4** - Scanning Electron Microscopy (SEM) images which shows the effects of a) fast printing set-up flattening of the extruded filament section and b) coarse printing set-up which causes macro pores

### 4.3 Influence of Filling density over acoustic properties

Figure 1 shows the sections of four samples where the resulting geometrical volumes are highlighted in red. The filling density in these volumes can be customised in the FDM set-up, while for the SLA, it is set as 100% by default: the SLA involves the solidification of liquid resin, which fills the geometrical domain entirely. Since this variable parameter may result in a significant variation in the acoustic performance, it is crucial to assess its influence on the difference between the experimental results from the expected ones (coming from the analytical and numerical design). For this reason, a final experimental analysis was run to determine the optimal filling density for FDM PETGg-based samples, keeping a slow-fine set-up (as assessed in the previous section). The filling percentages considered were 10%, 20%, 30%, 40%, and 50%, while all the other printing set-ups were kept as for the previous experimental analysis (including Printing Quality=Fine and Velocity=Slow). From the results shown in Figure 5, the samples which experimentally present higher correspondence with the analytical curve are those having a filling density of 30%, 40%, and 50%, while those with 10% and 20% filling density exhibit  $\alpha_n$ -peak too damped (especially in the lower frequency range). Therefore, the impact of infill density on the resulting volumes within the coiled-up resonator geometry is not negligible; the minimum filling density for acceptable results seems to be 30%.

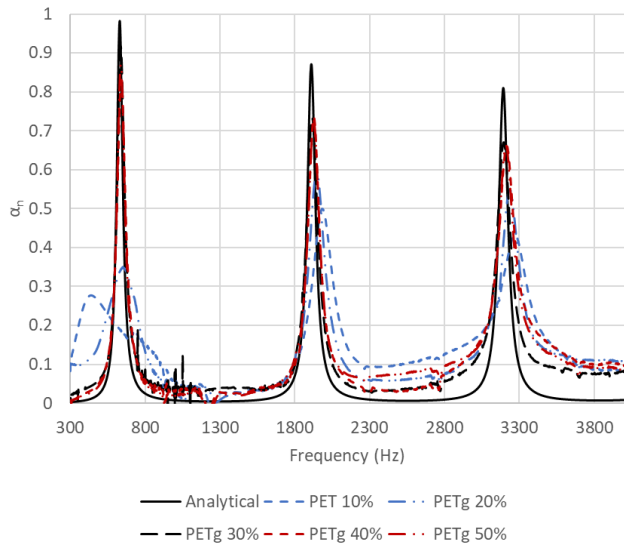


**Figure 5** – Comparison among the specimens fabricated with the five filling density settings (10%, 20%, 30%, 40%, 50% for PETG and 10%) and the prediction model.

## 5. CONCLUSIONS

Among the samples obtained with various 3D printing techniques and various constituent materials, FDM PETG represents a cheaper and less refined sample, which, however, can achieve the same acoustic performance as SLA resin (which is more expensive and requires more post-processing) by selecting the optimal printing configuration.

Our parametric and comparative study determined an optimal and cost-effective 3D printing set-up (slow-fine combined with infill density  $\geq 30\%$ ) and material selection for the production of spiral resonators that better approximate the provisional analytical and numerical results. It is hoped that the methodology, which at the moment is related to the specific coiled-up resonator case study, could be extended to other acoustic metamaterials in future studies, considering carefully their geometrical features.

## 6. ACKNOWLEDGEMENT

This research was funded by the Ministero dell'Istruzione dell'Università e della Ricerca (Italy), within the project PRIN 2017, grant number 2017T8SBH9: "Theoretical modelling and experimental

characterisation of sustainable porous materials and acoustic metamaterials for noise control".

## 7. CITATIONS

- [1] M. Cingolani, G. Fusaro, and M. Garai, "The influence of thermo-hygrometric conditions on metamaterials' acoustic performance: an investigation on a 3-D printed coiled-up resonator," 2022, doi: [https://doi.org/10.3397/IN\\_2022\\_0428](https://doi.org/10.3397/IN_2022_0428).
- [2] G. Fusaro, X. Yu, F. Cui, and J. Kang, "Development of a metamaterial for acoustic and architectonical improvement of window design.," *Proc. 23rd Int. Conf. Acoust.*, vol. 2019-Septe, no. September, pp. 1977–1983, 2019, doi: 10.18154/RWTH-CONV-239567.
- [3] H. von Helmholtz, *Die Lehre von den Tonempfindungen als physiologische Grundlage für die Theorie der Musik [The Study of the Sensations of Tone as a Physiological Foundation for Music Theory]*, 1 ed. 1863.
- [4] A. Alomarah, S. H. Masood, and D. Ruan, "Metamaterials with enhanced mechanical properties and tuneable Poisson's ratio.," *Smart Mater. Struct.*, vol. 31, no. 2, p. 025026, 2022.
- [5] B. Assouar, B. Liang, Y. Wu, Y. Li, J.-C. Cheng, and Y. Jing, "Acoustic metasurfaces," *Nat. Rev. Mater.*, vol. 3, no. 12, pp. 460–472, Dec. 2018, doi: 10.1038/s41578-018-0061-4.
- [6] W. Johnston and B. Sharma, "Additive manufacturing of fibrous sound absorbers," *Addit. Manuf.*, vol. 41, no. February, p. 101984, May 2021, doi: 10.1016/j.addma.2021.101984.
- [7] D. H. Kim and G. H. Yoon, "Active acoustic absorption device using additive manufacturing technique for normal incident wave," *Appl. Acoust.*, vol. 178, Jul. 2021, doi: 10.1016/J.APACOUST.2021.108006.
- [8] M. Askari *et al.*, "Additive manufacturing of metamaterials: A review," *Addit. Manuf.*, vol. 36, Dec. 2020, doi: 10.1016/J.ADDMA.2020.101562.

- [9] J. Kennedy *et al.*, “The Influence of Additive Manufacturing Processes on the Performance of a Periodic Acoustic Metamaterial,” 2019, doi: 10.1155/2019/7029143.
- [10] M. R. Stinson, “The propagation of plane sound waves in narrow and wide circular tubes, and generalization to uniform tubes of arbitrary cross-sectional shape,” *J. Acoust. Soc. Am.*, vol. 89, no. 2, pp. 550–558, 1991.
- [11] M. Cingolani, G. Fusaro, G. Fratoni, and M. Garai, “Influence of thermal deformations on sound absorption of three-dimensional printed metamaterials,” *JASA*, vol. 151, no. 6, 2022, doi: 10.1121/10.0011552.
- [12] X. Yu, Z. Lu, T. Liu, L. Cheng, J. Zhu, and F. Cui, “Sound transmission through a periodic acoustic metamaterial grating,” *J. Sound Vib.*, vol. 449, pp. 140–156, 2019, doi: 10.1016/j.jsv.2019.02.042.
- [13] A. Magnani, C. Marescotti, and F. Pompoli, “Acoustic absorption modeling of single and multiple coiled-up resonators,” *Appl. Acoust.*, vol. 186, Jan. 2022, doi: 10.1016/J.APACOUST.2021.108504.
- [14] G. Fusaro *et al.*, “Investigation of the impact of additive manufacturing techniques on the acoustic performance of a coiled-up resonator,” *J. Acoust. Soc. Am.*, vol. 153, no. 5, pp. 1–12, 2023, doi: <https://doi.org/10.1121/10.0019474>.
- [15] G. Fusaro, X. Yu, J. Kang, and F. Cui, “Development of metacage for noise control and natural ventilation in a window system,” *Appl. Acoust.*, vol. 170, p. 107510, 2020, doi: 10.1016/j.apacoust.2020.107510.
- [16] S. Marburg and B. Nolte, *Computational Acoustics of Noise Propagation in Fluids: Finite and Boundary Element Methods*. New York: Springer, 2008.
- [17] *ISO 10534-2: 1998. Acoustics – Determination of sound absorption coefficient and impedance in impedance tubes – Part 2: Transfer function method*. International Organisation for Standardisation, 1998.
- [18] C. Morris, L. Bekker, M. R. Haberman, and C. C. Seepersad, “Design exploration of reliably manufacturable materials and structures with applications to negative stiffness metamaterials and microstereolithography1,” *J. Mech. Des. Trans. ASME*, vol. 140, no. 11, 2018, doi: 10.1115/1.4041251.
- [19] V. E. Kuznetsov, A. N. Solonin, O. D. Urzhumtsev, R. Schilling, and A. G. Tavitov, “Strength of PLA Components Fabricated with Fused Deposition Technology Using a Desktop 3D Printer as a Function of Geometrical Parameters of the Process,” 2018, doi: 10.3390/polym10030313.